

Deform 3D Simulation and Experimental Investigation of Fixtures with Support Heads

Muthu Mekala NATARAJAN*, Balamurugan CHINNASAMY**, Bovas Herbert Bejaxhin ALPHONSE***

*College of Engineering, Anna University, Department of Mechanical Engineering, College of Engineering, Guindy Campus, Anna University, Chennai- 600025, Tamil Nadu, India, E-mail: muthumekalagunalan@annauniv.edu

**College of Engineering Guindy, Anna University, Department of Mechanical Engineering, College of Engineering, Guindy Campus, Anna University, Chennai- 600025, Tamil Nadu, India, E-mail: balamurugan.c@annauniv.edu

***Department of Mechanical Engineering, Saveetha School of Engineering, SIMATS, Chennai-602105.Tamil Nadu, E-mail: bovasherbertbejaxhina.sse@saveetha.com

crossref <http://dx.doi.org/10.5755/j02.mech.29468>

1. Introduction

Thin-walled complex structures are commonly employed in industrial applications such as electronics and aerospace. Process milling is highly desired for complex geometry profiles with considerable deformation, which influences surface roughness. Many researchers have studied thin-walled structure milling and presented various methods for predicting and optimising deformation values [1 – 3]. The mathematical model and experimental findings are compared in this way to determine the error in surface roughness measurements. It has been demonstrated that using Finite Element Analysis (FEA) to simulate the Computer Numerical Control (CNC) milling process is more advantageous. Fixtures and jigs will greatly reduce deflection during the milling operation. Some academicians have proposed their own fixture architecture to reduce deflection during the milling process. Optimization techniques are often used for forecasting deflection values and optimising fixture configuration.

De Jun Cheng et al [1] studied the influence of thin plate surface roughness along the feed direction, predicting that spindle speed, depth of cut, transverse distance, and other parameters would all play a role. Artificial bee colony algorithm (ABC) was used to discover the cutting condition, which was confirmed by the experimental results. Yishu Hao and Yang Liu [2] developed a milling surface roughness model based on tool wear and deformation to mill thin-walled objects with complex forms. They used the composite design approach to test the findings, which has the lowest inaccuracy. Lopez de Lacall et al. [3] established a new diagnostics method for identifying milling problems when machining real geometries with problems that differed greatly from those found when end-milling at constant linear feeds. Zhun et al. [4] used regression analysis to predict surface roughness and evaluated milling stability when process damping and surface roughness were both included. To optimise milling parameters, they applied a genetic optimization method. Maria Jackson et al. [5] have studied that the effect of process parameters on face milling of super alloy and proven that the surface roughness value will be the best quality with the suggested process parameters. Maohua Xiao et al. [6] have studied that the influence of machining factors of turning on surface roughness using the Response Surface Methodology

(RSM) of Taguchi optimization Process. They examined the tool life by employing the optimal cutting criterion. M. Tomov [7] proposed a mathematical methodology for estimating surface roughness of industrial materials. They devised an approach for estimating surface roughness ratings based on statistical values. K. Venkata Rao [8] employed the Teaching learning-based optimization TLBO for the turn milling process of silicon bronze alloy. He experimented with five different speeds, feed rates, and cut depths and determined that the feed rate has a significant effect on the cutting tool. Jixiong Fe et al. [9] demonstrated and recommended using a moveable milling fixture to reduce distortion induced by thin-walled framework milling. Altintas et al. [10] presented a novel method for estimating milling stability lobes. The axial depth of cuts and spindle speeds may be calculated simply using a sequence of linear analytic formulas. Bao [11,12] et al. proposed a multi-location support technique to minimise deflection in the mirror milling of aircraft skin by modifying the position of support points. They estimated the deflection values using a milling force model. The FEM simulation was tested using the experimental data of milling force measurements [12]. Jin Lan et al. [13] investigated the association between deflection and help head positions using artificial neural networks. They optimised the support head placements to lessen the amount of deflection generated by milling circular and square plates. To avoid machine tool system intervention, Lu Junbai and Zhon Kai [14] demonstrated the usage of multi-location support heads and a tooling system. Xianghui Huang et al. [15] studied the effect of cutting speed on orthogonal cutting in high-speed milling of aluminium alloys. They used three-level simulations to study the effects of tool rake angle and feed rake angle and established it as a simulation proven. J. Montalvo-Urquiza et al. [16] explored milling process optimization with two case studies: work piece deformation and shape error, and tool wear. Zhang et al. [17] conducted a thorough investigation on the optimization of low-carbon milling process parameters. They conducted experiments to evaluate the effect of milling settings, and the best technique was discovered utilising the NSGA II algorithm as a multi-objective problem. J. H. Shaik and J. S. [18] studied the effect of milling parameters such as feed, cutting speed, and axial depth of cut on the performance characteristics of an aluminium work piece such as vibration level and sur-

face roughness. They developed an approach for decreasing tool vibration and, as a result, workpiece surface roughness. Thabadira et al. [19] conducted a statistical analysis of both physical and mathematical modelling of the M200 TS workpiece. Jiahao Shi et al. [20] milled a thin-walled plate with variable thickness, predicted the machining quality, and confirmed the accuracy with an experimental approach. Yuan Haiyang [21] et al. developed a milling force model to predict the residual stresses induced in the aluminium frame work piece. They verified the simulation results with the experimental results and make the model as a guidance for many deformation calculations. Surface roughness is important in the milling process because the deformations induced have a direct impact on the surface consistency. Xiujie Yue et al. [22] have investigated the impact of various tool geometry factors on machinability. Different milling parameters were used to create finite element models of the 7050-T7451 aluminium alloy. Milling's forming mechanism has been established. Ming Chen et al. [23] have revealed that the results showed that when the cutting speed increased, the cutting force initially increased and subsequently declined. The inflection point of cutting speed grew as the feed per tooth increased.

Most of researchers have worked on the end milling of thin-walled plates especially with the aluminium. They suggested various methods and procedure to control the deformation induced during the machining. But few of them only concentrate on the reduction in the surface roughness in terms of deformation. In this research, the deflection caused in the thin wall plate aluminium alloy 6061 was therefore anticipated using simulation and experimentally measured using a horizontal milling machine. Based on simulation performance, the support head positions for milling fixtures are projected and experimentally tested. The surface roughness measurement was carried out before and after the use of milling fixtures.

2. Materials and methods

Aluminium Al6061 plate was chosen for the milling technique due to the higher distortion during the machining phase. The chemical composition of Al6061 consists of aluminium around 96.85 % in weight. The remaining consists of Magnesium 0.9 %, Silicon 0.75 % Iron 0 %, Copper 0.3 % and balance others. Because of its weldability and formability, this material is extensively employed for most general-purpose applications. Its corrosion resistance and great strength make it an excellent material for structural and automotive applications, among others. The specimen utilized in this experiment is Al 6061, with dimensions of 100x100 mm² and a thickness of 5mm. The plate is clamped on all four sides as the boundary condition for the Finite Element Analysis. Table 1 shows the parameters and dimensions used in the milling operation. Based on the tabular values provided, DEFORM-3D was utilized to perform three-dimensional finite element analysis. DEFORM-3D is utilized for simulation due of its distinct properties, such as robustness and a powerful simulation engine. Milling creates additional deformation in thin-walled work components; hence jigs or fixtures are required to limit deformation in such parts. The experiment is carried out both with and without the use of a fixture with support heads. High carbon steel is utilized in the

manufacture of support heads.

3. Simulated analysis of the milling

The entire machining process was intended to be predictable with the help of the Deform 3D current tool utilization. This is a free and open simulation framework that forecasts machine tool dynamics, work material removal damage levels, and stress and displacement development. It must be done at the pre-processing stage by inputting the machining parameters of speed, feed, and depth of cut into the relevant Deform 3D fields. Using the imported solid model of fixture construction, the specimen and tool setup can be inserted. The Table 1 shows the physical properties of the specimen and the input parameters of machining conditions for the Aluminium alloy plates that were employed. The Fig.1 shows the CAD Drawing and Solid Model of fixture with the support head.

Table 1

Parameters of Aluminium plate for milling (L. N. Lopez de Lacalle et al. [3])

| Parameters | Dimensions |
|------------------------------|--------------------------|
| Length X Breadth X Thickness | 100 mm X 100 mm X 5 mm |
| Poisson Ratio, ν | 0.33 |
| Young's modulus | 69 GPA |
| Density | 2.7 gm/cm ³ |
| Cutting Teeth Number | 3 |
| Cutter radius, r | 5 mm |
| Feed rate per revolution | 0.05 mm/rev |
| Depth of Cut | 0.5 mm |
| Cutting force coefficients | |
| K_{tc} | 2577 Nmm ⁻² |
| K_{ac} | 386.27 Nmm ⁻² |
| K_{rc} | 1576 Nmm ⁻² |
| K_{te} | 18.41 Nmm ⁻¹ |
| K_{ae} | 29.22 Nmm ⁻¹ |

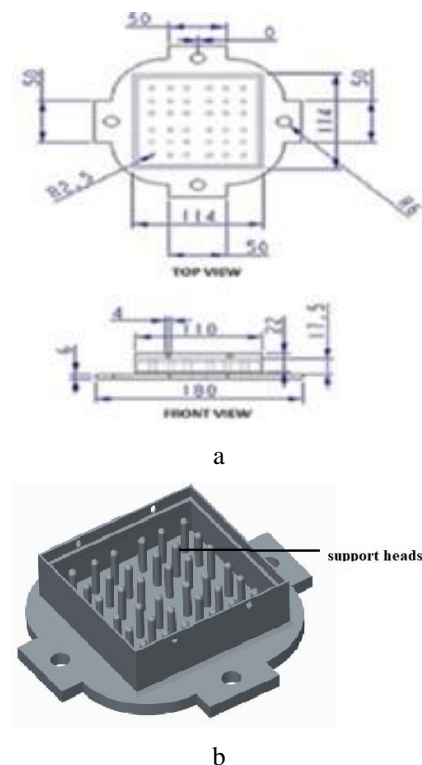


Fig. 1 Fixtures: a) CAD drawing of fixtures with support heads; b) solid model of fixture design

Fig. 2 depicts Positioning of work piece on the fixture and with the milling cutter. In the mesh generation procedure, the specimen model (15935 elements) and the milling cutter (4798 elements) were used. The material descriptions were collected from the material collection of Deform 3D. Load conditions, as well as tool and work piece location, have been described as boundary conditions. The clamping model was used to arrest the four sides of the specimen and the bolted end of the fixture, and the distributed form of nodal displacements was established. The displacements were calculated using simulated outputs in Deform 3D's post-processing stage. The displacement values of both specimens will be compared with and without the fixture configuration.

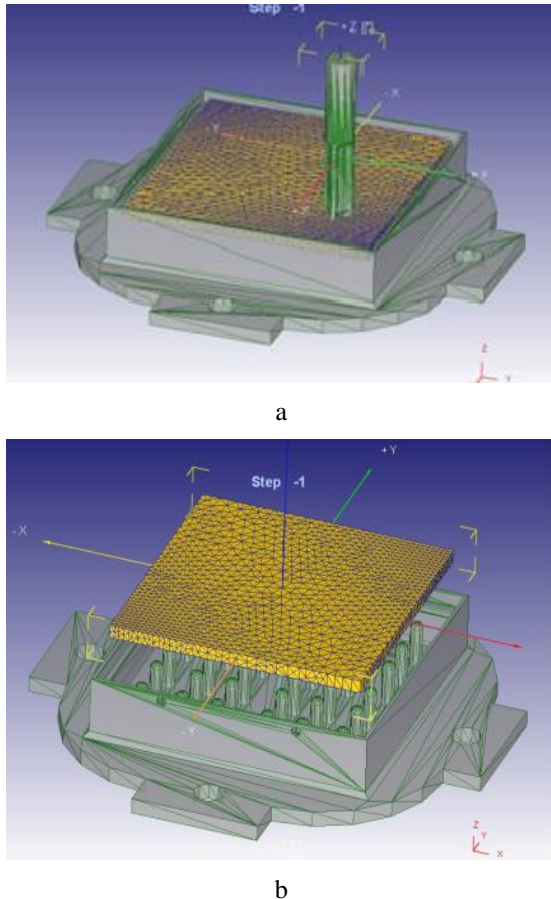


Fig. 2 Work piece in fixture: a) positioning of work piece on the fixture; b) combined positioning- fixture, specimen and milling cutter model

4. Experimental procedure and analysis

The experiment is carried On a Chetak 75M machining centre. Table 2 lists the specifications of the machining centre. The milling work piece was made of aluminium plate Al6061. Although it has great machining qualities, it is easily distorted during the machining process. The work piece is a $100 \times 100 \text{ mm}^2$ square plate with edge boundary constraints that are arrested on all sides. Table 1 discusses the milling process machining conditions, which are the same for both the simulation and experimental study. The milling operation is performed on the specified work piece in this paper with a load of 1000 N, a feed rate of 0.05 mm/rev-tooth, and a depth of cut of 0.5 mm (Fig. 3, b).

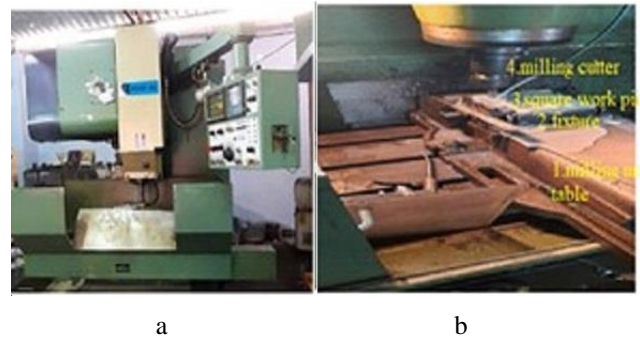


Fig. 3 a) CNC milling machine; b) aluminium plate held in vice

Table 2

Chetak 75 M Machining centre specifications

| Main Specifications | Chetak 75 MC |
|-----------------------------------|--------------------|
| Table Size ($L \times B$) | 950 x 520 mm |
| X-Axis Traverse | 762 mm |
| Y-Axis Traverse | 510 mm |
| Z-Axis Traverse | 510 mm |
| Spindle Nose Taper | BT-40 |
| Spindle Motor Power | 7.5 / 11 kw |
| Spindle Speed range | 60 - 6000 rpm |
| Rapid Rate X / Y / Z | 30 / 30 / 24 m/min |
| Automatic Tool changer Type (ATC) | Twin Arm Type |
| No. of Tool Stations in ATC | 24 Nos |

Fig. 3, b depicts an aluminium work piece gripped in a vice. The milling machine is programmed to turn at a rate of 1000 revolutions per minute. As illustrated in Fig. 4, the milling process is carried out in the direction of C1 corner point to C2 corner point. Based on simulation study with Deform 3D Software, the deformation generated in the plate is already anticipated for the applied load of 1000 N. The locations of the support heads are anticipated based on the software's predicted values, using the premise that where there is more deformation, a support head is required.

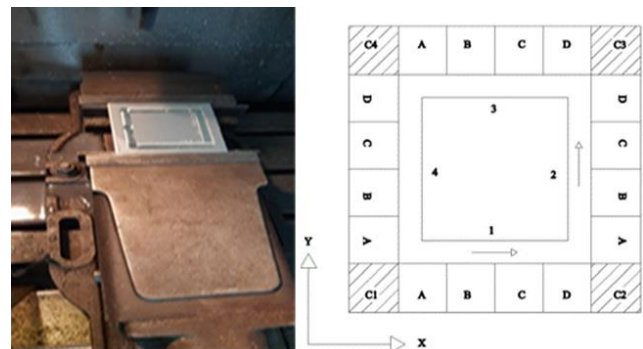


Fig. 4 Aluminium plate diagram: C1, C2, C3 and C4: corner points

The flow directed cutting series C1-C2 (A-B-C-D) was used. The support head is made of high carbon steel, which is noted for its cutting capacity, toughness, and wear resistance. Fig. 5 depicts an experimental model of a fixture with support heads. The experiment made use of nine support heads, each with a height of 10 mm, which was greater than the thickness of the thin-walled plate uti-

lized in the experiment. This fixture with support heads is fairly inexpensive, yet it looks to provide superior control during machining, increasing the stability of the work piece. The work piece is machined in a CNC milling machine in both circumstances, namely without and with the fixture arrangement. The surface roughness of the machined component is measured before and after using a fixture equipped with a portable Surface Roughness tester, the SURFTEST SJ-210. The movement of the diamond probe inductor detects the ups and downs of surface waviness which is denoted by "Ra." The average of the peaks has been assigned as "Ra" for this investigation.



Fig. 5 Experimental model of fixture with support heads

Fig. 6, a and b depict the visible impact of surface roughness. Fig. 6, b depicts a more pronounced improvement in surface finish. The surface roughness values obtained after the measurements are compared to justify the employment of the milling fixture with support heads. Fig. 7 illustrates the measurement of surface roughness at the cutting series.

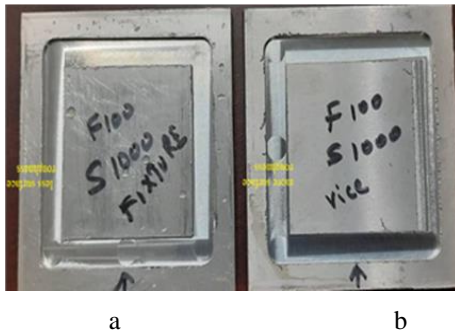


Fig. 6 Aluminium plate – machining: a) before; b) after the use of support heads

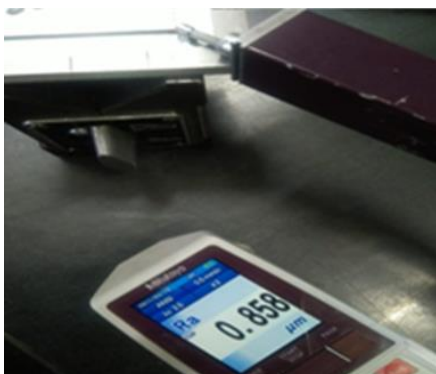


Fig. 7 Surface roughness measurement with SJ-210

5. Results and discussion

5.1. Deform 3D's displacement prediction

The iterative steps for the required machining conditions were computed using the Deform 3D version 11.0.2 simulation approach. Each section of the milling process in the experimental component was predicted before machining using the Deform 3D V.11.0.2 software approach. Using process settings and machining circumstances, the found specimen and tool model were used to animate the actual milling process in the post processing stage. These simulation results were presented in the form of component segments, with each segment going through roughly 110 iterations. As shown in Fig. 5, the milling process simulation displacement values were obtained with or without the fixture assembly. Table 3 displays the values of deformation. When the tool interacted with the specimen under the specified machining conditions and material attributes from the simulation tool's material library, the outputs were generated. Stress, strain, damage, strain rate, and displacement measurements can be measured at any node. In this situation, the Lagrangian approach of iteration was used, with a very precise degree of die movement. The displacements (Table 3) clearly illustrate that the maximum displacement values were attained for the milling without the usage of a fixture arrangement. The lower displacement values were reached by employing a novel aided fixture structure over the work table. The boundary conditions were met with this configuration, and the post-processing outcomes were judged to be better. As the tool moves along the X axis, the displacement increases to a maximum of 11.2 mm without the fixture and a minimum of 4.61 mm. With the addition of a fixture configuration in the simulation, a less displacement value of roughly 9.53 mm, corresponding to 11.2 mm displacement of step number 111, is obtained, with a 14.91 percent drop in deformation. Similarly, for the tool position at X-1, the greatest deformation is 7.13 mm and the minimum value is 6.98 mm, indicating a 2% decrease in deformation.

When it comes to the Y axis, the percentage reduction in deformation accounts or 34% reduction, which corresponds to a maximum deformation value of 9.83 mm. It shows a percentage decrease in distortion of up to 52% when the tool moves along the Y-1 axis.

The displacement values of the square plate milling operation with and without the fixture arrangement are shown in Fig 8. The maximum and minimum deformation values are highlighted for the axes along X, X-1, Y, and Y-1.

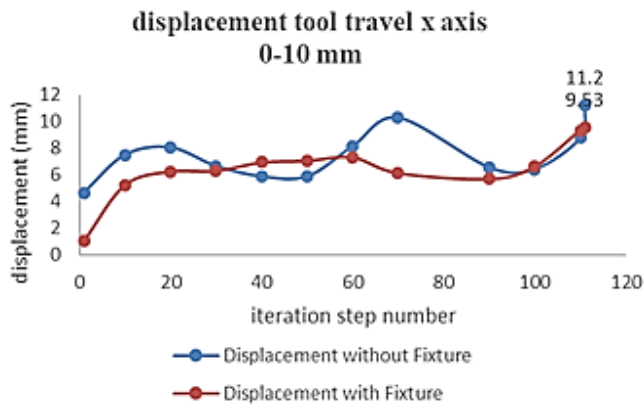
The use of fixtured attachment result in lower displacement values for 30-70 consecutive steps along the Y axis and 60-110 phase number along the Y-axis. The Y-1 axis provides the greatest drop in values greater than 50%.

Three phases in a row produced good results along the X-1 axis. Fig. 8, a through d exhibit graphical representations of displacements along the Y-1 axis with and without fixtures. The application of this can be demonstrated using the simulated values of the DEFORM-3D with and without the fixture arrangement.

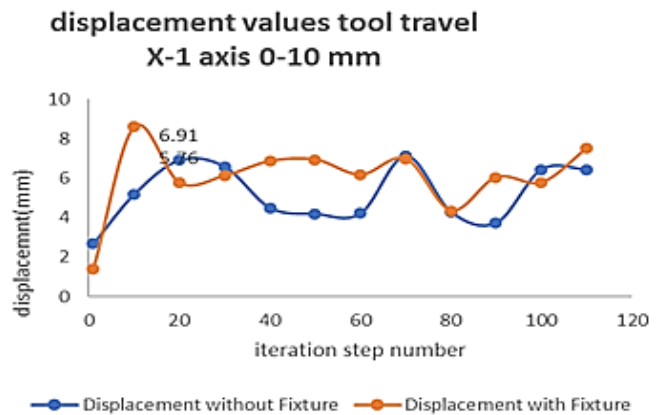
The Fig. 9 shows the simulated total displacement for the maximum displacement value for the axis X, X-1, Y and Y-1 with the absence and presence of fixture.

Simulation results of displacement values in the X, X-1, Y and Y-1 axes in Deform 3D

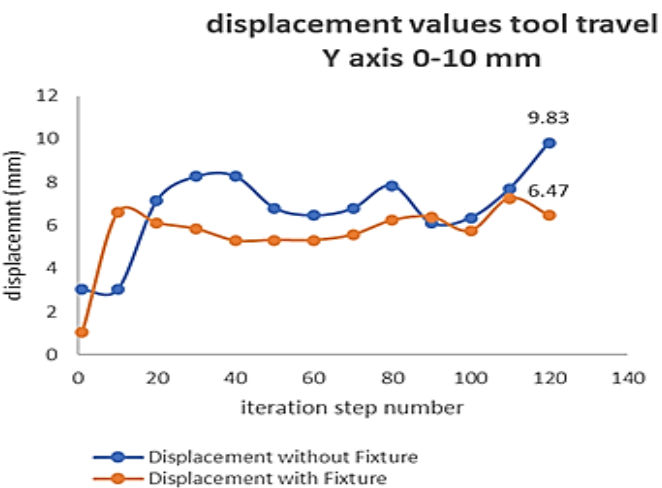
| X Axis 0-10 mm | | | X-1 0-10 mm | | | Y Axis 0-10 mm | | | Y-1 0-10 mm | | |
|----------------|------------------------------|---------------------------|-------------|------------------------------|---------------------------|----------------|------------------------------|---------------------------|-------------|------------------------------|---------------------------|
| Step No | Displacement without Fixture | Displacement with Fixture | Step No | Displacement without Fixture | Displacement with Fixture | Step No | Displacement without Fixture | Displacement with Fixture | Step No | Displacement without Fixture | Displacement with Fixture |
| 1 | 4.67 | 1.06 | 1 | 2.69 | 1.4 | 1 | 3.04 | 1.06 | 1 | 3.23 | 0 |
| 10 | 7.51 | 5.25 | 10 | 5.19 | 8.6 | 10 | 3.04 | 6.6 | 10 | 6.36 | 6.5 |
| 20 | 8.08 | 6.27 | 20 | 6.91 | 5.76 | 20 | 7.16 | 6.1 | 20 | 6.18 | 6.18 |
| 30 | 6.67 | 6.31 | 30 | 6.58 | 6.12 | 30 | 8.26 | 5.83 | 30 | 6.6 | 6.57 |
| 40 | 5.89 | 6.95 | 40 | 4.51 | 6.86 | 40 | 8.28 | 5.29 | 40 | 5.66 | 6.33 |
| 50 | 5.89 | 7.07 | 50 | 4.21 | 6.94 | 50 | 6.81 | 5.32 | 50 | 7.26 | 6.35 |
| 60 | 8.16 | 7.33 | 60 | 4.23 | 6.17 | 60 | 6.47 | 5.31 | 60 | 9.39 | 6.37 |
| 70 | 10.3 | 6.16 | 70 | 7.13 | 6.98 | 70 | 6.79 | 5.56 | 62 | 13.4 | 6.37 |
| 80 | 8.85 | 6.1 | 80 | 4.3 | 4.36 | 80 | 7.85 | 6.23 | 70 | 7.42 | 8 |
| 90 | 6.56 | 5.71 | 90 | 3.76 | 6.05 | 90 | 6.12 | 6.39 | 80 | 7.42 | 6.39 |
| 100 | 6.44 | 6.64 | 100 | 6.45 | 5.78 | 100 | 6.36 | 5.74 | 90 | 7.42 | 6.7 |
| 110 | 8.81 | 9.36 | 110 | 6.45 | 7.52 | 110 | 7.71 | 7.26 | 100 | 7.42 | 6.41 |
| 111 | 11.2 | 9.53 | - | - | - | 120 | 9.83 | 6.47 | 110 | 7.42 | 6.41 |



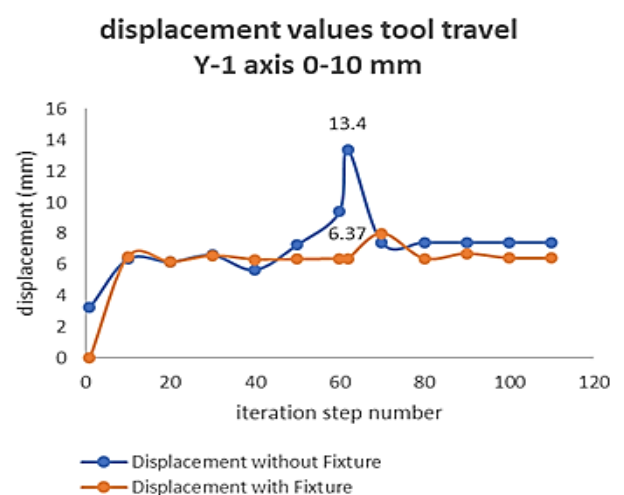
a



b



c



d

Fig. 8 a) X; b) 1; c) Y; d) Y-1 axis displacement values from the Deform 3D modelling tool

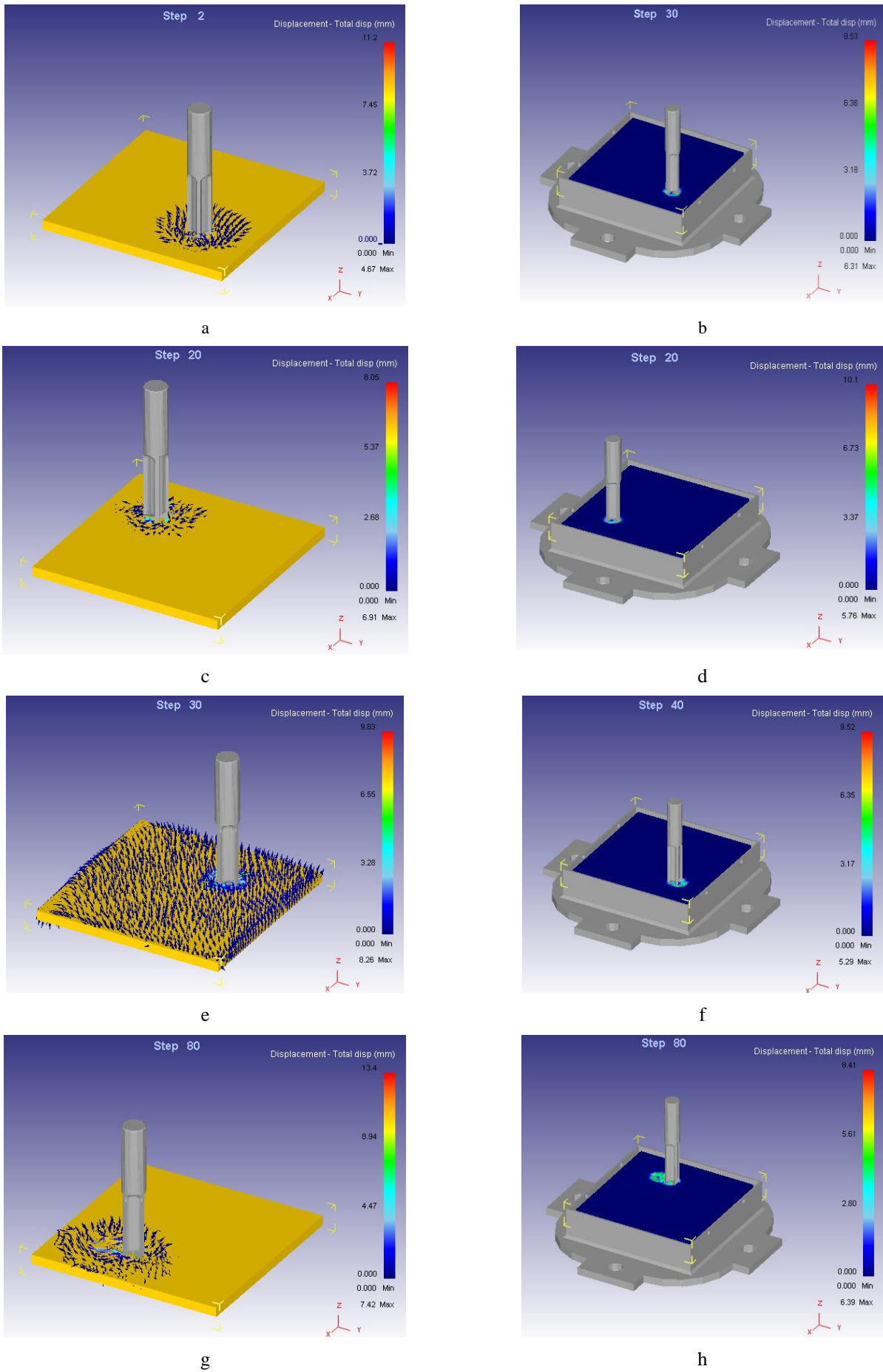


Fig. 9 ISO Plots of displacement simulations of the milling in: a) X axis without fixture; b) X axis with fixture; c) X-1 axis without fixture; d) X-1 axis with fixture; e) Y axis without fixture; f) Y axis with fixture; g) Y-1 axis without fixture; h) Y-1 axis with fixture

5.2. Surface roughness and the effect of the fixture

During the milling operation, some cutting forces were applied to the working surface by the tool and the specimen. The supporting cylindrical rod was inserted in the fixture, as illustrated in Figs. 1 and 2, with a uniform spacing between them. The displacements in the Deform 3D simulation results were computed using different iteration stages. As indicated in Table 4, these simulation results are matched to the surface roughness experimental outputs. The milling procedure was carried out in the usage of fixture position has resulted in an increase in productivity of around 30%. The specimen's bottommost surfaces can be protected under dispersed resistive load situations by using this fixture. In the machined specimen, the four separate cutting profiles have been considered as segments as C1-C2, C2-C3, C3-C4, and C4-C1. Using the fixture connection, the minimum roughness values were determined. In the machining slot of C1-C2, a minimum surface roughness of 0.28 μm was achieved (Fig. 10). The minimum roughness of 0.77 to 0.79 μm has been registered in the majority of the milling slots. Hence the surface roughness is reduced by the percentage in ranging from 10.8% (corresponding to position-to-position D) and 27.2% cor-

responding to position A. However, in the absence of a fixture, a greater amount of roughness has been confirmed. In the machining slot C2-C3, the range of decrease in surface roughness is from 8.6% (corresponding to position D) to 22.4% (corresponding to position A). Similarly, for the slot C3-C4, 2.13 (corresponding to position B) % to 19.77% (corresponding to position C) decrease in the surface roughness is achieved. For C4 to C1, the decrease is percentage is from 6.4% for position A and 13.1% for position D.

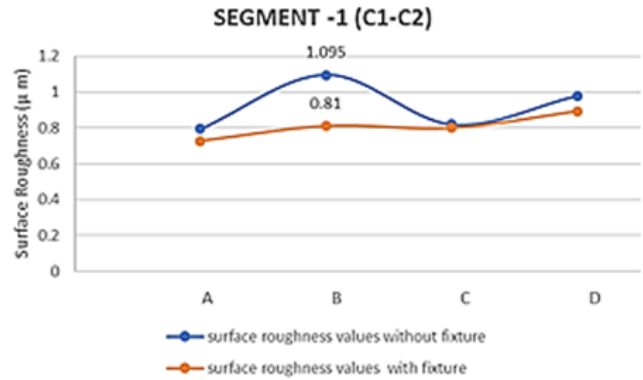

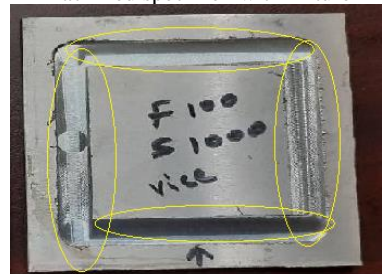


Fig. 10 Surface roughness segment (C1-C2)

Table 4

Surface roughness values (μm) on slots and corners with and without a fixture

| Position | Surface roughness (μm) | | Position | Surface roughness (μm) | | Specimen samples |
|-------------------|-------------------------------------|---|---------------------------|-------------------------------------|--|--|
| | Without fixture | With fixture | | Without fixture | With fixture | |
| Corner | | | Segment-3 (C3-C4) | | |  Machined specimen with fixture |
| C1 | 1.125 | 0.791 | A | 0.679 | 0.780 | |
| C2 | 0.989 | 0.770 | B | 1.313 | 1.285 | |
| C3 | 0.699 | 0.847 | C | 0.986 | 0.791 | |
| C4 | 0.749 | 1.095 | D | 1.031 | 0.851 | |
| Average | 0.8905 | 0.87575 Reduction by 1.74 % | Average | 1.00225 | 0.92675 Reduction by 6.12 % |  Machined specimen without fixture |
| Segment-1 (C1-C2) | | | Segment-3 (C4-C1) | | | |
| A | 0.794 | 0.728 | A | 1.130 | 0.936 | |
| B | 1.095 | 0.81 | B | 1.065 | 1.035 | |
| C | 0.819 | 0.799 | C | 1.095 | 1.041 | |
| D | 0.979 | 0.892 | D | 5.1.295 | 0.869 | |
| Average | 0.92175 | 0.80725 Reduction by 19.28 % | Average | 0.8625 | 0.97025 No reduction | |
| Segment-2 (C2-C3) | | | Average (μm) | Average (μm) | | |
| A | 1.025 | 0.776 | Corner | 0.8905 | 0.8755 | |
| B | 0.809 | 0.799 | Segment C1-C2 | 0.92175 | 0.80725 | |
| C | 1.105 | 0.904 | Segment C2-C3 | 0.97775 | 0.84825 | |
| D | 0.972 | 0.914 | Segment C3-C4 | 1.00225 | 0.92675 | |
| Average | 0.97775 | 0.84825 Reduction by 15.18 % | Segment C4-C1 | 0.8625 | 0.97025 | |
| | | | Average | 0.9377 | 0.8886 Reduction by 11.44 % | |

The elimination of the initial milling slot in each corner has been noticed more, and it needs to be strengthened by positioning the fin-like support system at the bottom of the specimen. The milling segment - 4 (C4-C1) has more waviness of 1.13 to 1.295 μm due to the modulation of feed rate due to resistive forces against that specific nodal point displacements. An average surface roughness of 0.9377 μm is obtained without the machining without the fixture, but with the fixture arrangement the surface

roughness value is 0.886 μm . Hence the average surface roughness reduction is around 11.44%.

5. Conclusions

Deform 3D simulation and experimental investigations have been performed to obtain the surface roughness and deformation of thin wall aluminium alloy 6061 plate while machining in End-milling machine with the use

of work holding device of fixture with and without support heads. The cylindrical protruding support heads in fixture are arresting the displacement of workpiece at several nodal points and hence improve the surface roughness. In this research, the following conclusions have been arrived:

1. From the deform 3D's displacement prediction the percentage of reduction in displacements with support heads are 14.91%, 2%, 34% and 52% along X, X1, Y and Y1 axis respectively.

2. The presence of a fixture with support heads resulted in a significant reduction in surface roughness ranging 1.74% at corner position and 19.28% at segment 1 position.

3. The average surface roughness reduction is around 11.44%.

This study can be further carried out with other types of profiles of support heads by varying boundary conditions for further reduction of displacement and hence improve the surface roughness of aluminium thin wall pate machining in end-milling machine for several industrial applications.

References

- De Jun Cheng; Feng Xu; Sheng Hao Xu; Chun Yan Zhang; Sheng Wen Zhang; Su Jin Kim.** 2020. Minimization of surface roughness and machining deformation in milling of Al alloy thin walled parts, *International Journal of Precision Engineering and Manufacturing*, p.1597-1613. <https://doi.org/10.1007/s12541-020-00366-0>.
- Yishu Hao; Yang Liu.** 2017. Analysis of milling surface roughness prediction for thin-walled parts with curved surface, *Int. J. Adv. Manuf. Technology* 93: 2289–2297. <https://doi.org/10.1007/s00170-017-0615-4>.
- Lopez de Lacalle, L. N.; Lamikiz, A.; Sanchez, J. A.; Fernandez de Bustos, I.** 2006. Recording of real cutting forces along the milling of complex parts, *Mechatronics* 16: 21–32. <https://doi.org/10.1016/j.mechatronics.2005.09.001>.
- Lida Zhu; Baoguan Liu; Hongyu Chen.** 2017. Research on chatter stability in milling and parameter optimization based on process damping, *Journal of Vibration and Control* 24(12): 2642-2655. <https://doi.org/10.1177/1077546317692159>.
- Jackson, M.; Baskar, N.; Sabarish, R.; Mohan Raj, S.; Annis Ahmed, A.** 2020. Productivity and quality improvement by optimization of milling parameters of superalloy, *Materials Today* 33: 3491-3496. <https://doi.org/10.1016/j.matpr.2020.05.415>.
- Maohua Xiao; Xiaojie Shen; You Ma; Fei Yang; Nong Gao; Weihua Wei; Dan W.** 2018. Prediction of Surface roughness and optimization of cutting parameters of stainless steel turning based on RSM, *Hindawi Mathematical Problems in Engineering*, 15 p. <https://doi.org/10.1155/2018/9051084>.
- Tomov, M; Kuzinovski, M; Cichosz, P.** 2016. Development of mathematical models for surface roughness parameter prediction in turning depending on the process condition, *International Journal of Mechanical Sciences* 113(2016): 120-132. <https://doi.org/10.1016/j.ijmecsci.2016.04.015>.
- Rao, K. V.** 2019. A novel approach for minimization of tool vibration and surface roughness in orthogonal turn milling of silicon bronze alloy, *Silicon* 11: 691–701. <https://doi.org/10.1007/s12633-018-9953-6>.
- Jixiong Fei; Bin Lin; Juliang Xiao; Mei Ding; Shuai Yan; Xiaofeng Zhang; Jin Zhang.** 2018. Investigation of moving fixture on deformation suppression during milling process of thin-walled structures, *Journal of Manufacturing Processes* 32: 403-411. <https://doi.org/10.1016/j.jmapro.2018.03.011>.
- Altintas, Y.; Budak, E.** 1995. Analytical prediction of stability lobes in milling, *Annals of the CIRP* 44(1): 357-362. [https://doi.org/10.1016/S0007-8506\(07\)62342-7](https://doi.org/10.1016/S0007-8506(07)62342-7).
- Yan Bao; Renke Kang; Zhigang Dong; Xianglong Zhu; Changrui Wang; Dongming Guo.** 2017. Multi-point support technology for mirror-milling of aircraft skins, *Materials and Manufacturing Processes* 3(9): 996-1002. <https://doi.org/10.1080/10426914.2017.1388519>.
- Bao, Y; Zhi Gang Dong; Ren Ke Kang; Zhao Li; Yi Chu Yuan.** 2016. Milling force and machining deformation in mirror milling of aircraft skin, *Advanced Materials Research* 1136: 149–155. <https://doi.org/10.4028/www.scientific.net/amr.1136.149>.
- Jin Lan; Bin Lin; Tian Huang; Ju-Liang Xiao; Xiao-Feng Zhang; Ji-Xiong Fei.** 2017. Path planning for support heads in mirror-milling machining system, *The International Journal of Advanced Manufacturing Technology* 91: 617–628. <https://doi.org/10.1007/s00170-016-9725-7>.
- Lu Junbai, L; Zhou Kai.** 2011. Multi-point location theory, method, and application for flexible tooling system in aircraft manufacturing, *Int. J. Adv. Manuf. Technology* 54: 729–736. <https://doi.org/10.1007/s00170-010-2974-y>.
- Xianghui Huang; Jinyang Xu; Ming Chen; Fei Ren.** 2020. Finite element modeling of high-speed milling 7050-T7451 alloys, *Procedia Manufacturing* 43: 471–478. <https://doi.org/10.1016/j.promfg.2020.02.186>.
- Montalvo-Urquizo; Niebuhr, C.; Schmidt, A.; Villarreal-Marroquin, M. G.** 2018. Reducing deformation, stress, and tool wear during milling processes using simulation-based multiobjective optimization, *The International Journal of Advanced Manufacturing Technology* 96: 1859–1873. <https://doi.org/10.1007/s00170-018-1681-y>.
- Zhang, C; Li W; Jiang P; Gu P.** 2017. Experimental investigation and multi-objective optimization approach for low-carbon milling operation of aluminum, *Proceedings of the Institution of Mechanical Engineers, Part C: Journal of Mechanical Engineering Science* 231(15): 2753-2772. <https://doi.org/10.1177/0954406216640574>.
- Jakeer Hussain Shaik; Srinivas, J.** 2017. Optimal selection of operating parameters in end milling of Al-6061 work materials using multi-objective approach, *Mechanics of Advanced Materials and Modern Processes* 3: 5. <https://doi.org/10.1186/s40759-017-0020-6>.

19. **Tlhabadira, I.; Daniyan, I. A.; Masu, L.; VanStaden, L. R.** 2019. Process design and optimization of surface roughness during M200 TS milling process using the Taguchi method, *Procedia CIRP* 84: 868-873.
<https://doi.org/10.1016/j.procir.2019.03.200>.
20. **Jiahao Shi; Jian Gao; Qinghua Song; Zhanqiang Liu; Yi Wan.** 2017. Dynamic deformation of thin-walled plate with variable thickness under moving milling force, *Procedia CIRP* 58: 311-316.
<https://doi.org/10.1016/j.procir.2017.03.329>.
21. **Yuan Haiyang; Wu Yunxin; Gong Hai; Wang Xiaoyan.** 2015. A milling deformation model for aluminum alloy frame-shaped workpieces caused by residual stress, *Mechanika* 21(4): 313-322.
<http://dx.doi.org/10.5755/j01.mech.21.3.9176>.
22. **Zhang Ping; Xiujie Yue; Han Shuangfeng; Song Ailing; Li Baoshun; Yu Xiao.** 2020. Experiment and simulation on the high-speed milling mechanism of aluminum alloy 7050-T7451, *Vacuum* 182.
<https://doi.org/10.1016/j.vacuum.2020.109778>.
23. **Xianghui Huang; Jinyang Xu; Ming Chen; Fei Ren;** 2020. Finite element modeling of high-speed milling 7050-T7451 alloys, *Procedia Manufacturing* 43: 471-478.

M. M. Natarajan, B. Chinnasamy, B. H. B. Alphonse

DEFORM 3D SIMULATION AND EXPERIMENTAL INVESTIGATION OF FIXTURES WITH SUPPORT HEADS

S u m m a r y

Thin-walled aluminium components are used in many sectors, including construction and aerospace. They are more resistant to deformation when subjected to a larger amount of grinding. As a result, the stability of the work components deteriorates, and the surface roughness rises. This paper suggests using a well-designed fixture with support heads to reduce deformation caused by square thin-walled aluminium plate milling. The support heads of the recommended fixture system are made of high-carbon steel. The milling experiment is carried out in a CNC Machining centre using machining parameters identical to those used in DEFORM 3D-Simulation. Surface roughness is measured using the SURFTEST SJ-210 portable Surface Roughness tester in two scenarios: without and with fixtures used during the milling operation. Surface roughness values are lowered by a minimum of 3% to a maximum of 19% as a result of using this fixture with support heads to reduce deformation. As a consequence, the suggested fixture with support head has been shown to decrease distortion in thin-walled aluminium plates.

Keywords: CNC milling, surface roughness, fixture, deform 3D.

Received July 16, 2021

Accepted April 08, 2022



This article is an Open Access article distributed under the terms and conditions of the Creative Commons Attribution 4.0 (CC BY 4.0) License (<http://creativecommons.org/licenses/by/4.0/>).